
A GC-SSIM-CRDS System: Coupling a Gas Chromatograph with a Cavity Ring-Down Spectrometer for Onboard Twofold Analysis of Molecular and Isotopic Compositions of Natural Gases during Ocean-Going Research Expeditions

Brandily Christophe ^{1,*}, Le Cuff Nolwenn ², Donval Jean-Pierre ², Guyader Vivien ², De Prunele Alexis ², Cathalot Cecile ², Croguennec Claire ², Caprais Jean-Claude ¹, Ruffine Livio ²

¹ Ifremer, REM/EEP-Laboratoire Environnements Profonds, Centre de Brest, ZI Pointe Du Diable, CS100, F-29280 Plouzané, France

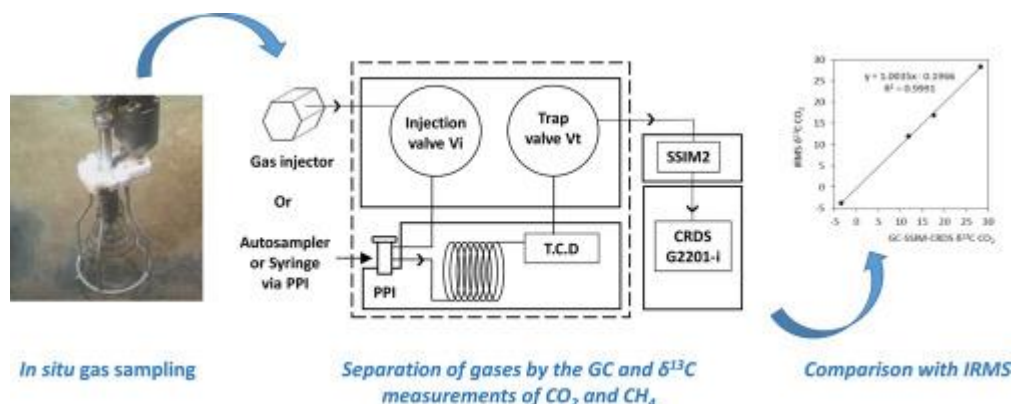
² Ifremer, REM/GM-Laboratoire Cycles Géochimiques et Ressources, Centre de Brest, ZI Pointe Du Diable, CS100, F-29280 Plouzané, France

* Corresponding author : Christophe Brandily, email address : christophe.brandily@ifremer.fr

Abstract :

Carbon dioxide (CO₂) and methane (CH₄) are two climate-sensitive components of gases migrating within sediments and emitted into the water column on continental margins. They are involved in several key biogeochemical processes entering into the global carbon cycle. In order to perform onboard measurements of both the molecular and stable carbon isotope ratios ($\delta^{13}\text{C}$) of CH₄ and CO₂ of natural gases during oceanic cruises, we have developed a novel approach coupling gas chromatography (GC) with cavity ring-down spectroscopy (CRDS). The coupled devices are connected to a small sample isotope module (SSIM) to form a system called GC-SSIM-CRDS. Small volumes of natural gas samples (<1 mL) are injected into the GC using a headspace autosampler or a gas-tight syringe to separate the chemical components using a Shincarbon ST packed column and for molecular quantification by thermal conductivity detection (TCD). Subsequently, CO₂ from the sample is trapped in a 7 mL loop at 32 °C before being transferred to the CRDS analyzer for sequential determination of the stable carbon isotope ratios of CH₄ and CO₂ in 24 min. The loop is an open column (without stationary phase). This approach does not require the use of adsorbents or cooling for the trapping step. Optimization of the separation step prior to analysis was focused on the influence of two key separation factors 1) the flow of the carrier gas and 2) the temperature of the oven. Our analytical system and the measurement protocol were validated on samples collected from gas seeps in the Sea of Marmara (Turkey). Our results show that the GC-SSIM-CRDS system provides a reliable determination of the molecular identification of CH₄ and CO₂ in complex natural gases, followed by the stable carbon isotope ratios of methane and carbon dioxide.

Graphical abstract



Highlights

► We present a coupled analytical system associating gas chromatography and cavity ring down spectroscopy (GC-SSIM-CRDS) for natural gas analyses. ► The analytical system allows fast onboard analyses of both molecular composition of natural gases and stable carbon isotope ratios of methane and carbon dioxide in 24 min. ► The GC-SSIM-CRDS was optimized and validated with samples from natural gas seeps. ► The GC-SSIM-CRDS is a decision-making tool suitable to refining sampling strategy of gases when characterizing seep areas and is a useful analytical system for scientific purposes.

Keywords : Coupled analytical technique, cavity ring-down spectroscopy, carbon dioxide, gas chromatography, methane, molecular composition, natural gases, onboard analysis, stable carbon isotope ratio

39 *1 Introduction*

40 Methane (CH₄) and carbon dioxide (CO₂) are among the most abundant greenhouse
41 gases on Earth [14] and are strongly responsible for climate change. The major sources of
42 atmospheric methane are wetlands, landfills, livestock farming, hydrocarbon-field production,
43 as well as natural seepages from geologic structures including marine emissions. During the
44 2008–2017 decade, the total emissions was estimated between 550 to 600 Tg CH₄ yr⁻¹ with a
45 mean estimation of 7 Tg CH₄ yr⁻¹ for marine geological emissions [1–4]. Human activity is a
46 major source of carbon dioxide responsible for the imbalance of this compound in the
47 atmosphere. Global antropogenic fossil CO₂ emissions was estimated at 38.0 Gt in 2019 [5].

48 In marine environments, methane and carbon dioxide are also key molecules that are
49 encountered in hydrothermal systems and at cold seeps [6]. Their sources as well as their
50 mechanisms of formation are different from the processes that take place at these different
51 environments. These ecosystems are characterized by emissions of fluids rich in methane and
52 hydrogen sulphide that sustains the development of specific chemosynthetic communities [7–
53 10]. Methane is either the product (methanogenesis) or the substrate (methanotrophy) of

54 biogeochemical redox reactions within both the sedimentary and the water columns [11–15].
55 Oceanic methane can also be of abiotic origin, and may be generated from reduction of carbon
56 dioxide or serpentinization processes [10–13].

57 Although natural CO₂ seepages are found in sedimentary basins, it is mainly
58 encountered in volcanic and hydrothermal areas [16–18]. In nature, the four main processes that
59 generate CO₂ are the decomposition of organic matter at low temperature, the oxidation of
60 hydrocarbons either via thermal reactions or by microbial sulfate reduction, the decomposition
61 of carbonates and degassing from the mantle [19]. In the case of hydrocarbon-derived CO₂, its
62 $\delta^{13}\text{C}$ is influenced by the abundance of the hydrocarbons and their isotopic signature under
63 reservoir conditions [20–22]. In sedimentary basins, positive or higher $\delta^{13}\text{C}$ values could be
64 related to an inorganic source of CO₂ generated from the thermal breakdown of carbonate rocks
65 [22]. In contrast to methane, carbon dioxide seepages from sedimentary environments have
66 been less investigated [23].

67 Earth scientists analyze molecular and isotopic composition of natural gases to interpret
68 their origin. The origin of natural gases containing (CH₄ or C1), ethane (C₂H₆ or C2), propane
69 (C₃H₈ or C3) and carbon dioxide (CO₂), is commonly interpreted using binary genetic diagrams
70 of $\delta^{13}\text{C}$ -C1 versus C1/(C2 + C3) [24], $\delta^{13}\text{C}$ -C1 versus $\delta^2\text{H}$ -C1 [25,26] and $\delta^{13}\text{C}$ -C1 versus $\delta^{13}\text{C}$ -
71 CO₂ [27]. A revision of these empirical diagrams has been done and it is based on more than
72 20000 samples [28]. It includes the genetic fields for primary microbial gases from CO₂
73 reduction and methyl-type fermentation, secondary microbial gases generated during petroleum
74 biodegradation, thermogenic (ie thermal cracking of organic matter in deep-hydrocarbon
75 reservoirs) and abiotic gases. These diagrams are key tools to provide interpretations of gas
76 origins.

77 The wide range of CO₂ and CH₄ sources and their potential mixing can lead to a broad
78 range of $\delta^{13}\text{C}$ signature; and at cold seeps characterized by a large number of gas seeps over

79 hundreds of square meters to square kilometers, themselves characterized by numerous gas
80 streams. Understanding gas transport and geochemical-transformation processes requires a
81 multifold sampling strategy to collect many gas samples over a wide range of molecular and
82 isotopic compositions.

83 Accordingly onboard measurement of $\delta^{13}\text{C-CH}_4$ and $\delta^{13}\text{C-CO}_2$, together with the
84 molecular composition of the gases, can be valuable as a decision-making tool on
85 oceanographic cruises to quickly characterize gas seep sites and also for scientific purposes to
86 define the gas emissions with the binary genetic diagrams $\delta^{13}\text{C-C1}$ versus $\delta^{13}\text{C-CO}_2$. For
87 instance, such information will help in targeting the more interesting samples and refining the
88 sampling resolution at gas emission sites, and thus avoiding sampling gas streams having close
89 molecular and isotopic compositions of CH_4 and CO_2 [29]. This was our primary incentive for
90 the development of the GC-SSIM-CRDS. In the following paragraph, we describe the
91 specifications for the design of the GC-SSIM-CRDS and its detailed description, the
92 optimization of the method, and the evaluation of its accuracy and precision against well-proven
93 analytical methods.

94 Isotope-Ratio Mass Spectrometry (IRMS) is the most prevalent, reliable and accurate
95 analytical technique used to measure the $\delta^{13}\text{C}$ of C-bearing compounds, including methane and
96 carbon dioxide. Regardless of the compounds, the end product measured from this technique is
97 the relative abundance of $^{12}\text{CO}_2$ and $^{13}\text{CO}_2$ [30–32]. Accordingly, the analysis of compounds
98 other than carbon dioxide, e.g. methane, requires its conversion into CO_2 via a combustion step
99 before entering into the mass detector. However, an Isotope-Ratio Mass Spectrometer is relative
100 expensive, requires significant space for its installation, in an environment devoid of strong
101 vibrations, and therefore is not suitable for fast onboard analysis during oceanic expeditions.
102 cavity ring down spectroscopy (CRDS) has been proposed as an alternative technique to IRMS

103 [33–35], and is based on the absorption rate of a near-infrared laser light confined within a
104 closed optical cavity. The analyzer is compact and easy to operate, provides a fast and low-drift
105 signal, and can be used both in laboratory and in field (e.g. shipboard analysis). The instrument
106 has been designed for continuous gas sampling through an optical cavity. The CRDS technique
107 has been used for isotopic measurements of carbon dioxide, methane and water vapor at
108 atmospheric concentrations [33]. However, applications in the field of deep-sea fluid systems
109 like cold seeps to support the sampling strategy while providing reliable and accurate data
110 remains scarce. The main issue to unlock such applications is the determination of the possible
111 influence of chemical compounds between each other and to understand how this affects the
112 measurement.

113 One of the major constraints related to CRDS applied to deep-sea environments is the
114 limitation in the volume of samples that can be collected and the heterogeneity in concentration.
115 Indeed, methane concentration in pore water ranges from nmol L^{-1} to mmol L^{-1} , while this
116 compound can represent more than 99 mol% of the total gas composition [16,36]. Similar
117 constraints hold true for carbon dioxide. These constraints have to be taken into consideration
118 for the development of analytical methods, more particularly for the injection step of discrete
119 samples. In the case of oceanic samples, injection using manifold and syringe, or based on the
120 headspace technique are usually the most appropriate [37–39]. Moreover, previous studies have
121 shown that analyses from CRDS instruments can exhibit bias in measurements due to
122 interference from other natural gases on the laser absorption. As an example, the presence of
123 H_2S can cause interference on $\delta^{13}\text{C-CO}_2$ [40] which consequently leads to an overestimated
124 depletion in the measured $\delta^{13}\text{C}$. The effect of air compounds (nitrogen, N_2 ; oxygen, O_2 ; argon,
125 Ar; water, H_2O ; and helium, He) also affects significantly the determination of CO_2 and CH_4
126 concentrations with the CRDS [38,39]. Other recent studies have shown biases induced from
127 ethane on the $\delta^{13}\text{C-CH}_4$ [37,41]. Some of these studies proposed specific isotopic corrections

128 derived from a calibration step with known standards. Thus, cross sensitivity is measured by
129 creating a gas-dilution series to control the concentration of the compounds responsible for
130 interference. For instance, to correct the interference of ethane on $\delta^{13}\text{C-CH}_4$, the concentration
131 of ethane needs to be precisely determined as there are cross-interferences with the
132 concentration of H_2O , CO_2 and CH_4 . Often, multiple corrections are needed to obtain reliable
133 and accurate $\delta^{13}\text{C-CH}_4$ values. According to the manufacturer of the CRDS analyzer used in
134 this study, methane at a concentration higher than 500 ppm could also be an interfering
135 compound on the isotopic measurement of $\delta^{13}\text{C-CO}_2$ [42].

136 Here, we present a coupled system consisting of a CRDS analyzer and a gas
137 chromatograph (GC) for upstream separation of the chemical compounds present in the
138 analysed gases followed by molecular analysis, and prior to the $\delta^{13}\text{C}$ analysis. This system
139 enables easy separation of CH_4 and CO_2 in a complex matrix of compounds commonly present
140 in natural gases using either a headspace device, a gas injector [43] or by applying direct manual
141 injection with a syringe. A similar system coupling a gas chromatograph with a CRDS analyser
142 has been described once in the literature [44] to measure stable carbon isotope ratios of methane,
143 ethane and propane. The coupled devices are used 1) to directly and rapidly determine the
144 molecular composition of the natural gases, followed by 2) for fast analysis of the $\delta^{13}\text{C}$ of
145 methane and carbon dioxide. The influence of the amount of non-methane hydrocarbons,
146 carbon dioxide and hydrogen sulfide on the reliability of the method has been studied.

147

148 **2 Materials and Methods**

149 **2.1 Description of the coupled GC-SSIM-CRDS system**

150

151 The system is composed of a modified gas chromatograph (GC) Agilent 6850 (Agilent
152 Technologies, Santa Clara, CA, USA) coupled with the SSIM-CRDS (Fig.1 and 2). The isotopic

153 analyzer used for this study is a G2201-i Cavity Ring-Down Spectrometer (CRDS) coupled
154 with a Small Sample Isotope Module (SSIM), both from Picarro®, USA. The CRDS G2201-i
155 can measure both $\delta^{13}\text{C-CH}_4$ and $\delta^{13}\text{C-CO}_2$. The SSIM is a sample management peripheral
156 designed to accommodate small gas volumes (< 20 mL) prior to injection into the analyzer.
157 This device is commonly used to inject gases via gastight syringes, samples Tedlar® bags or
158 directly by connecting a bottle onto it. The SSIM is composed of a 20 mL sample chamber, five
159 solenoid valves, an external vacuum pump, and an internal pressure sensor. It requires a
160 pressurized supply of zero air dry gas. Every SSIM-CRDS analysis begins with two purge
161 cycles of the SSIM chamber using vacuum and zero air supply to remove any memory effects
162 between samples. Before and after each purge, the vacuum pump evacuates the SSIM chamber.
163 Once ready for injection, the SSIM chamber stays under vacuum and a gas sample can be
164 delivered into the chamber by vacuum transfer. Once the injection of the gas sample into the
165 SSIM chamber is complete, the Coordinator software from Picarro closes the solenoid valve in
166 relation with the injection port and opens the one connected to the cavity to deliver the sample
167 into the CRDS cavity and measure the $\delta^{13}\text{C-CH}_4$ and $\delta^{13}\text{C-CO}_2$. This system allows an easy
168 way to accommodate and dilute samples.

169 The SSIM could also induces a dilution of the sample with zero air. For instance, if a
170 sample of 5 mL at atmospheric pressure is injected inside the SSIM, the pressure inside the cell
171 will be about $5/20 \times 760$ Torr. The zero air will be added inside the cell to allow a good transfer
172 of the gas to the CRDS. If the pressure of zero air is about 900 torr, this will create a dilution
173 of about 4.7. Further information on the use of the SSIM is described in supplementary material.

174 According to the manufacturer, isotopic measurements should be made in well-defined
175 ranges of methane concentrations. The so-called High Range (HR) is applied when the methane
176 concentration ranges between 10 and 1000 ppm, while the High Precision range (HP) is most
177 suitable for methane concentration ranging from 1.8 to 12 ppm. The GC has been modified to

178 meet the requirement for individual separation of CH₄ and CO₂ from natural gases after the
179 determination of their molecular composition. It is composed of an injector, a Shincarbon ST
180 (80/100 mesh and 2 m x 3 mm) column, a μ thermal conductivity detector (μ TCD) and a
181 trapping loop of 7 mL. There are three possible ways to inject samples into the Agilent 6850
182 gas chromatograph using either a gas injector [43] of 5mL connected to the gas valve (Vi), a
183 gas-tight syringe to be inserted into the purge packed injector (PPI) or a headspace auto-sampler
184 connected to the PPI. Simultaneously, direct injection into the SSIM-CRDS can be performed
185 using a gas-tight syringe (Fig.1 and 2). Environmental gas samples analyzed in this study were
186 injected directly inside the SSIM port by the use of a gas-tight syringe or by the use of the gas
187 injector to fill the 1 mL injection loop of the Vt valve. The amount of gas injected inside the
188 injection loop was calculated using the ideal gas law and controlled by decreasing gently the
189 pressure of the gas inside the gas injector with the vacuum pump of the CRDS and by measuring
190 the pressure with a sensor.

191 The optimized analytical conditions applied to the GC are given in Table 1. Two
192 softwares, Open lab from Agilent and Coordinator, were used for the GC and the SSIM-CRDS,
193 respectively, to set and control the instrument parameters for analysis. A homemade subroutine
194 was created for communication between the GC and SSIM-CRDS.

195 Although helium is commonly used as the carrier gas for natural gas analysis using GC-
196 μ TCD as its thermal conductivity is much higher than that of hydrocarbons, it significantly
197 affects the measurement of $\delta^{13}\text{C-CO}_2$ with the CRDS due to collisional line broadening and
198 Dicke narrowing effects [39]. Accordingly, nitrogen gas as a carrier has been chosen to limit
199 these effects. The influence of nitrogen as a carrier gas on the influence of the GC performance
200 was also studied and discussed.

201

202 2.2 *Measurement principle*

203

204 First, the molecular composition of the gas sample is determined from classical GC-
205 μ TCD analysis. Next, the injected gas sample is transferred into a trapping loop installed on the
206 gas-switching 8-port valve (Vt). This valve is pneumatically activated, and the 7 mL loop which
207 is an open column is used to trap and store the CO₂ while the $\delta^{13}\text{C}$ -CH₄ measurement is taking
208 place. This system does not require the use of adsorbent or cooling for trapping CO₂. By
209 switching the Vt valve from one position to another, the loop can be connected to the injection
210 port of the SSIM device to deliver the gas sample under vacuum transfer. While a $\delta^{13}\text{C}$ -CH₄
211 measurement starts, CO₂ is still retained on the column. Once CH₄ has been transferred to the
212 CRDS, the Vt valve is switched back to its initial position and wait for the elution of CO₂. Once
213 eluted, CO₂ is trapped and stored inside the loop until the opening of the SSIM. Finally the CO₂
214 is injected inside the SSIM by vacuum transfer.

215 Valve Vt is regulated at 32 °C to avoid any ambient temperature variations and to
216 maintain good repeatability of the trapping. Fig. 3 shows the flow path for trapping and the
217 subsequent $\delta^{13}\text{C}$ analysis of methane and carbon dioxide by switching the valve from one
218 position to another.

219

220 2.3 *Reference Materials and calibration procedures*

221

222 Certified $\delta^{13}\text{C}$ -CH₄ and $\delta^{13}\text{C}$ -CO₂ gas standards were used for the isotopic calibration
223 of the SIIM-CRDS analyzer alone and in the coupled configuration with the GC-SSIM-CRDS.
224 Four commercial certified $\delta^{13}\text{C}$ -CH₄ gas standards, supplied by Isometric Instruments (Victoria,
225 Canada), were used (Table 2). These gas standards are composed of methane diluted in
226 hydrocarbon-free air. The calibration of carbon dioxide was performed using four commercial

227 standards from -40.1‰ to -7.1‰ diluted into hydrocarbon-free air and with a given uncertainty
228 of less than $\pm 0.5\%$ (Table 2).

229 The CRDS was first calibrated directly without the coupling system by injecting 5
230 replicates 5 mL of certified $\delta^{13}\text{C-CH}_4$ gas standards inside the inlet port of the SSIM with the
231 help of gastight syringes (Hamilton) and Tedlar® sampling bags (Restek). Due to the
232 concentration of the CH_4 standards at 2500 ppm and the dilution occurring with the SSIM, the
233 volume of 5 mL of CH_4 was chosen to have approximately up to 500 ppm of CH_4 detected at
234 the CRDS. This allows to make molecular and isotopic measurements in the middle of the
235 concentration range of the HR mode. The same procedure was applied for the certified $\delta^{13}\text{C-}$
236 CO_2 gas standards by injecting 5 replicates of 500 μL of the standard at -7.12, -13.51 and -22.62
237 ‰ and 50 μL of the standard at -40.1‰ to reach a CO_2 concentration of approximately 1000
238 ppm inside the CRDS. The $\delta^{13}\text{C-CH}_4$ and $\delta^{13}\text{C-CO}_2$ calibration with the coupling system was
239 achieved by the use of the headspace autosampler (Dani HSS86.50, Italy) and a 1 mL injection
240 loop. Compounds introduced inside the GC were trapped by the use of the loop trap and the Vt
241 valve and then transfer to the SSIM-CRDS. The $\delta^{13}\text{C-CH}_4$ certified standards were realized by
242 flushing 10 mL sealed vials with certified isotopic standard (table 2) at 500 mL min^{-1} . Only the
243 certified $\delta^{13}\text{C-CO}_2$ standard at -40.1‰ was realized differently by injecting 1 mL of the certified
244 standard (from a Tedlar® bag) inside vials previously flushed with zero air. As the Autosampler
245 introduce a dilution inside the vial, because a pressurization step is needed for the filling of its
246 injection loop, it was not used to analyze the samples. The autosampler was used for the
247 automatization of the calibration procedure of the whole analytical line going from separation
248 of compounds, trapping of the gas of interest and isotopic analysis into the CRDS.

249 A preliminary test was made to check the stability of the response signal of the CRDS
250 analyzer prior to analysis. Thus, 10 repeated injections of 5 mL of the $\delta^{13}\text{C-CH}_4$ standard at -
251 38.3‰ and 500 μL of the $\delta^{13}\text{C-CO}_2$ standard at -23.9‰ were performed directly into the SSIM

252 once the cavity reached its working temperature of 45 °C. This test was achieved with separate
253 runs for CH₄ and CO₂.

254 2.4 *In Situ gas sampling*

255
256 Natural gas samples were collected during the Marsitecruise [16,29] in the sea of
257 Marmara, at water depth ranging from -22 m to -1273 m, with a gas-bubble sampler (PEGAZ)
258 [36,45]. These samples were used for validating the system by comparing our measured $\delta^{13}\text{C}$ -
259 CH₄ values with the results from Isolab b.v (The Netherlands) using a GC-C-IRMS. The
260 PEGAZ sampler was designed to collect gas bubbles and preserve the sample at the *in situ*
261 pressure. Aliquots of gas were then subsampled at lower pressure of 2 to 4 bars in 12 mL pre-
262 evacuated vials from Labco[®] by connecting the PEGAZ sampler to a gas transfer system [46].
263 The remaining gases were stored in metallic containers of 100, 200 or 1000 mL.

265 2.5 *Molecular gas analysis*

266 The present study is mainly focus on the separation of CH₄ and CO₂ follow by $\delta^{13}\text{C}$
267 analysis with a SSIM-CRDS. In order to achieve good isotopic measurement, it is necessary to
268 preliminary know the composition of gases from the samples to control the amount of gas
269 injected inside the GC to avoid overloading on the GC column or inside the CRDS. We have
270 chosen to work with samples with known concentrations of gases and previously analyzed. The
271 concentration of these gases are given in this study to give informations about the complexity
272 of the gas mixture from environmental samples. Molecular composition analysis was carried
273 out both on-board and at the “Laboratoire des Cycles Géochimiques et ressources” (LCG) at
274 Ifremer. A gas chromatograph μGC R3000 from SRA equipped with a μTCD and a PoraPlot U
275 capillary column was used on-board to determine nitrogen, oxygen, methane to hexane and

276 carbon-dioxide concentrations. Hydrocarbons at low concentrations in the samples (< 1%-mol)
277 were analyzed at the LCG using an Agilent 7890 A gas chromatograph equipped with a 32 m,
278 0.32 mm Porapak Q column. The uncertainty in the measurements was of $\pm 2\%$ for methane
279 and carbon dioxide concentrations, and $\pm 4\%$ for the heavier hydrocarbons.

280

281 *2.6 Performance of the GC for separation and analysis of CH₄ and CO₂*

282

283 In order to optimize the separation of CH₄ and CO₂ with the nitrogen carrier gas, an
284 experimental design has been conducted. The idea was to have enough time between the two
285 peaks to allow enough time for the Vt valve to trap CH₄ and come back to its initial position
286 before trapping CO₂. The gas volume of each peak were studied. As the carrier gas flow and
287 the oven temperature have a direct influence on the resolution and peak shapes, they were
288 selected as factors for the experimental design. The Doehlert matrix [47] has been used on
289 several types of chromatography techniques. It is useful to optimize the separation between
290 species [48]. This matrix has been used in the separation of H₂, O₂, N₂ and CH₄ on Shincarbon
291 ST column [49]. The application of the experimental design uses basically three steps: realized
292 the designed experiments, estimate the coefficients in a mathematics model, predicting the
293 responses and checking the model adequacy. The aim of this application was to find the best
294 compromise which allows a good separation between the peaks of CO₂ and CH₄ on the GC
295 regarding the carrier gas flow and the oven temperature. The number of experiments required
296 for the Doehlert experimental design (N) is given by $N = n^2 + n + n_0$, where n and n_0 are
297 respectively the number of variables and n_0 is the number of center points. In our case, the n_0
298 value was fixed at 3; thus, with two factors (gas flow and oven temperature). The number of
299 experiments was 9. The carrier gas flow was studied at five levels (6, 7, 8, 9, 10 mL min⁻¹) and

300 temperature at three levels (161, 180 and 199°C). Three responses were determined; peaks
301 width of the two gases and the difference of retention time between the compounds. Further
302 information on the experimental design is provided in the supplementary material. All the
303 calculations related to the experimental design were performed with the statistical software
304 NemrodW. The significance of each coefficient was determined by the Student test. Hence, it
305 is assumed that the residues are randomly distributed with a constant variance and the observed
306 response data points follow normal distribution.

307 Once the parameters of the carrier gas flow and the oven temperature defined, the GC
308 configuration was evaluated for separation of CO₂ and CH₄ in a complex gas mixture (1ml of
309 CO₂ 5% CLM-3783-10 + 1 mL of a gas mixture of 1% of C1 to C5 in nitrogen from Air Liquide)
310 by injecting this 2 mL of this mixture inside the gas injector of the GC. The injected volume on
311 the GC is 1mL. CO₂ and the C1-C5 mixture have also been injected separately for peaks
312 identification.

313 A study was also made to determine the limits and compromises in term of gas
314 concentrations in which the GC-SSIM-CRDS is able to manage for consecutive (CH₄ then CO₂)
315 or individual runs. The limit of detection for both gases were evaluated using a mixture of CH₄
316 and CO₂ (2% in air balance from Messer) at different pressures and by using the 0.1 mL
317 injection loop of Vi.

318

319 *2.7 Statistics used to assess the effect of concentration variation on the $\delta^{13}\text{C}$ -*

320 *CH₄*

321 Method accuracy was evaluated by measuring bias and precision. The maximal bias
322 (MB) was defined as being 0.8‰ as we believe that a precision of <1‰ allows to reliably
323 estimate the gas sources or the level of mixing. The measurement of trueness was expressed as
324 follows:

$$325 \quad \text{Bias}(\%) = \frac{|z - \text{ref}|}{\text{ref}} * 100$$

326 With z being the average value obtained from five series of duplicate measurements and ref ,
 327 the certified $\delta^{13}\text{C-CH}_4$ value. Precision was estimated by the relative standard deviation
 328 calculated from the intra and inter-series variances. Finally, the method was validated in terms
 329 of accuracy control if it satisfies the following constraints:

$$330 \quad \text{ref} + \text{MB} > z + 2s \quad \quad \quad \text{ref} - \text{MB} < z - 2s$$

331 The bias is considered negligible to estimate the uncertainty (U) at $k = 2$ with normalized error
 332 $(NE) < 2$.

$$333 \quad NE = \frac{|z - \text{ref}|}{\sqrt{s^2 + u_{\text{ref}}^2}} \quad \quad U = 2 * \sqrt{s^2 + u_{\text{ref}}^2}$$

334 With s being the standard deviation of the series, u_{ref} is the uncertainty of the reference value,
 335 and k the coverage factor in the uncertainty estimates for a 95% confidence interval.

337 **3 Results and discussion**

338 **3.1 CRDS stability and injection repeatability**

339
 340 Regarding the preliminary test, results show that the CH_4 and CO_2 concentration
 341 measurements from the ten consecutive injections remain relatively constant, with a mean value
 342 of 539 ppm and 624 ppm, and a relative standard deviation RSD of 0.7% and 0.6% for CH_4 and
 343 CO_2 , respectively (see supplementary). While methane concentration at the detector remains
 344 stable over the entire injection series, the $\delta^{13}\text{C-CH}_4$ varies significantly for the first five
 345 injections with an amplitude of 0.9‰ for the two tested standards T-iso1 (-38.3‰ for $\delta^{13}\text{C-}$
 346 CH_4) and CLM-3781 (-22.7‰ for $\delta^{13}\text{C-CO}_2$), and such behavior has already been pointed out

347 by the manufacturer [42] in case of hyphenated systems such as the G2121-i CRDS analyzer
348 coupled with a combustion module (CM-CRDS). In such a case, they recommended to calculate
349 the standard deviation of six consecutive analyses, and then to check that the obtained value is
350 under a specific threshold depending on the instrument. The G2201-i instrument uses a
351 wavelength monitor with a line-locking algorithm to detect and analyzed the ^{13}C and ^{12}C of the
352 CH_4 or CO_2 . This means that the CRDS analyzer needs a certain time to run and stabilize the
353 signal. As the instrument is working with the SSIM to deliver a small volume of gas inside the
354 cavity, the CRDS is then working in a closed system without continuously analyze ambient air
355 and detect CH_4 and CO_2 for its line-locking detection and positioning. Therefore, the first five
356 measurements were automatically discarded from our measurement series.

357

358 *3.2 Influence of the gas concentration on $\delta^{13}\text{C}-\text{CH}_4$ and $\delta^{13}\text{C}-\text{CO}_2$*

359

360 As described previously, the G2201-i analyzer was designed to measure the $\delta^{13}\text{C}-\text{CH}_4$
361 and $\delta^{13}\text{C}-\text{CO}_2$ at specific ranges of concentrations. Fig. 4 shows the $\delta^{13}\text{C}-\text{CH}_4$ measurements in
362 the concentration range recommended by the manufacturer, which is the HR mode (between 12
363 to 1000 ppm of methane). This test was achieved directly by the used of the SSIM-CRDS
364 without the GC.

365

366 Clearly, there is an influence of the methane concentration on $\delta^{13}\text{C}-\text{CH}_4$ when moving
367 towards the lowest concentration limits of the HR mode. For methane concentrations below 25
368 ppm, the measured $\delta^{13}\text{C}-\text{CH}_4$ varies significantly, and several values fall outside the certified
369 accuracy of the standards (in the range of -38.1 to -38.5‰). This may be explained by the so-
370 called optical extinction due to scattering processes [50,51]. Nevertheless, these results are in

371 agreement with the precision provided by the manufacturer with a standard deviation (σ_p) of
372 0.55‰ for $\delta^{13}\text{C-CH}_4$ [42]. As the GC-SSIM-CRDS was designed to analyze mainly methane-
373 concentrated gas samples, its use at concentrations close to the lowest limit of the HR mode is
374 unlikely. In order to achieve reliable measurements, the isotopic analysis of methane was
375 carried out in HR mode with methane concentration higher than 25 ppm. The HR mode was
376 also assessed in the concentration range between 50 to 1000 ppm (Table 3) with a maximum
377 bias (MB) value of 0.8‰, the method is validated for all four isotopic standards and in a range
378 of 55 to 1011 ppm of CH_4 injected within the CRDS cavity. The averaged values of measured
379 $\delta^{13}\text{C-CH}_4$ fall within the uncertainty range of the certified materials, and below the maximal
380 bias defined in this study.

381 Fig. 5 shows the variation of $\delta^{13}\text{C-CO}_2$ with its concentration ($[\text{CO}_2]$) and for direct
382 injection inside the SSIM-CRDS. For each certified standard, there is a linear relationship
383 between $\delta^{13}\text{C-CO}_2$ and $1/[\text{CO}_2]$. The measured $\delta^{13}\text{C-CO}_2$ is enriched in ^{13}C with increasing
384 $[\text{CO}_2]$. Such physical effect was reported in the literature [39], and was explained as the
385 differences between $^{12}\text{CO}_2$ and $^{13}\text{CO}_2$ regarding adsorption/desorption process of the light
386 circulating through the cavity. The observed effects was described to give positive $\delta^{13}\text{C}$ bias
387 correlated with increasing CO_2 concentration. However, such linearity clearly shows that it is
388 possible to link the $\delta^{13}\text{C}$ with $1/[\text{CO}_2]$. Comparison between measured and certified $\delta^{13}\text{C-CO}_2$
389 was carried out for different CO_2 concentrations (Fig.6). Previous works have shown the
390 possibility to linearize the $\delta^{13}\text{C-CO}_2$ versus the variation of $1/[\text{CO}_2]$ with a GG2201-i analyzer
391 [52]. We then studied the influence of the variation of $[\text{CO}_2]$ on the typical plot use to correct
392 the $\delta^{13}\text{C-CO}_2$ (ie $\delta^{13}\text{C-CO}_2$ measured vs $\delta^{13}\text{C-CO}_2$ certified)

393 Equation (1) was used to correct measured $\delta^{13}\text{C-CO}_2$ values in accordance to certified
394 values. The figure also shows the effect of $[\text{CO}_2]$ variation on the correlation curves. Both the
395 slope and the intercept could be linearized regarding the concentration (Fig. 7) to give

396 respectively equation (1.1) and equation (1.2). These equations are then used to obtain the final
 397 equation (1.3) which is the $\delta^{13}\text{C-CO}_2$ corrected from $[\text{CO}_2]$ measured inside the analyzer for a
 398 range of concentration in accordance with the specifications from Picarro (380-2000 ppm) and
 399 for $\delta^{13}\text{C-CO}_2$ ranging from -7.2 to -40.1 ‰.

$$400 \quad \delta^{13}\text{C} = \delta^{13}\text{C measured} * A_N + B_N \quad (1)$$

401

402 with A_N the slope and B_N the intercept of the normalization correction.

403

$$404 \quad A_N = a/[\text{CO}_2] + b \quad (1.1)$$

405

406 with a and b the slope and intercept for A_N , respectively.

407

$$408 \quad B_N = \alpha/[\text{CO}_2] + \beta \quad (1.2)$$

409

410 with α and β the slope and intercept for B_N , respectively.

411

$$412 \quad \delta^{13}\text{C} = \delta^{13}\text{C measured} * (a/[\text{CO}_2] + b) + (\alpha/[\text{CO}_2] + \beta) \quad (1.3)$$

413

414 with $a = 2.5814$, $b = 1.0147$, $\alpha = 2211.6$ and $\beta = -1.8389$ and $\delta^{13}\text{C measured}$ (‰) and $[\text{CO}_2]$ the
 415 CO_2 concentration measured at the CRDS in ppm.

416

417 *3.3 Performance of the GC separation for trapping of CH₄ and CO₂.*

418

419 The carrier flow of 6 mL min⁻¹ and the oven temperature of 184°C obtained from the
420 Doehlert optimization procedure allow a nice separation of CH₄ and CO₂ on the Shincarbon ST
421 column. These two conditions were selected to have enough time for the system to trap the CH₄
422 and send it to the CRDS while the CO₂ was still retained and passing through the Shincarbon
423 ST column. The volumes of each of the two gases were used as responses in the Doehlert matrix
424 by multiplying the peaks width with the total gas flow at the end of the GC system. Total gas
425 flow was given by the addition of the carrier gas flow of 6 mL min⁻¹ and the detector flow of 9
426 mL min⁻¹. With a carrier gas flow of 6 mL min⁻¹ and the oven temperature of 184°C, peaks
427 width were well constrained during the Doehlert optimization procedure giving 0.26 min for
428 CH₄ and 0.34 min for CO₂.

429 The GC system was evaluated for the separation of CH₄ and CO₂ in a mixture of C1 to
430 C5 compounds CH₄ and CO₂ are well separated from a matrix of gases from C2 to C5. Retention
431 times of CH₄ and CO₂ are respectively of 3.0 and 4.1 min. It was not possible to elute and
432 separate gases > C3. C2 was eluted by the use of thermal and N₂ flow gradients presented on
433 Figure 8. To avoid any little accumulations of C3 to C5 (as these are present at lower
434 concentrations) which can progressively change the GC retentions of CH₄ and CO₂, it has been
435 chosen to regenerate the column during 1h at a carrier gas flow of 20 mL min⁻¹ and with an
436 oven temperature of 280 °C every 24 samples. No variation of retention times were observed.
437 The CRDS analyzer needs approximately 10 min to run a sample and so the global time of
438 analysis of CH₄ followed by CO₂ is about 24 min.

439 As previously mentioned, N₂ was chosen as a carrier gas thanks to its compatibility with
440 CRDS. The main influence of choosing nitrogen as a carrier gas compare to helium is the lack

441 of contrast regarding the detection of CO₂ as they have similar thermal conductivity [53].
442 According to the literature, at 20°C, the respective thermal conductivity of He, N₂, CH₄ and
443 CO₂ are respectively of 150, 24, 35 and 17 mW mK⁻¹. In this configuration, the limits of
444 detection were evaluated for CH₄ and CO₂. The limits of detection for CH₄ and CO₂ with N₂ is
445 respectively of 6 ppm and 30 ppm. The limits of detection for CH₄ and CO₂ with Helium are
446 1.4 ppm and 2.1 ppm. As the isotopic measurements of δ¹³C-CH₄ and CO₂ have to be operate
447 in a valid range of concentrations inside the CRDS, we recommend to first measure the
448 concentrations of gases and then to make isotopic measurements. The coupling system
449 developed in this study allows to control the amount of gas injected on the GC column easily
450 by the use of a gas injector. It is possible to decrease the amount of gas loaded on the injection
451 loop by decreasing gently the pressure inside the gas injector by the use of the CRDS pump
452 directly connected onto it and a needle valve. The amount of a gas injected on the column has
453 a direct influence on the peak width and on the concentration detected at the CRDS. We have
454 defined compromises in terms of maximum injected gas amounts by measuring the peaks
455 volumes of each gas and by checking the CRDS gas concentrations measured. Table 4 shows
456 the range of concentrations of CH₄ and CO₂ which have to be injected inside the GC-SSIM-
457 CRDS system for appropriate δ¹³C measurements with the CRDS.

458 The lowest limit of methane concentration which can be injected on the GC prior to
459 δ¹³C-CH₄ analysis on the CRDS is about 0.14% in HR mode. As the HP mode of the CRDS
460 use a concentration of CH₄ low as 1.8 ppm it is potentially possible to work with gas sample as
461 methane concentration as low as 0.010%. Compromises have been made by evaluating the
462 maximum amount of gases tolerated on the column which limit peaks width of the two
463 compounds and also correspond to the range of concentrations needed for valid isotopic
464 measurements. The most important factor was the defined range of concentration needed for
465 the CRDS. The range of concentrations which permit sequential isotopic analysis for CH₄ and

466 CO₂ is low. Due to this narrow range and to the high differences of concentrations between the
467 two gases in environmental samples, $\delta^{13}\text{C-CH}_4$ and $\delta^{13}\text{C-CO}_2$ were mostly measured
468 individually. The main limitation of the system is that a minimum concentration of 1.1% of
469 CO₂ is needed for the $\delta^{13}\text{C-CO}_2$ measurement as the CRDS needs a minimum concentration of
470 380 ppm of CO₂. In perspective to improve the system, it is possible to increasing the trapping
471 volume to study the possibility of transferring more gas to the CRDS. A work on GC parameters
472 can also be done to increase the volume of the injection loop of the Vi valve to increase the
473 amount of gas injected for lower CO₂ concentration. The study of the influence of the gas
474 concentration of CO₂ on the $\delta^{13}\text{C-CO}_2$ have shown a good linear relation between the $1/[\text{CO}_2]$
475 and the $\delta^{13}\text{C-CO}_2$. Some of these measurements were done at lower concentration than 380
476 ppm. For instance, the certified $\delta^{13}\text{C-CO}_2$ standard of -7.2 ‰ was analyzed at a concentration
477 of 323 ppm with still a good linear relation between $\delta^{13}\text{C-CO}_2$ and the inverted gas
478 concentration. This also means that it is possible to work to extend the limit of the CO₂
479 concentration needed for $\delta^{13}\text{C-CO}_2$ measurements and to analyze lower concentrated gases with
480 the coupling system.

481 *3.4 Calibration of the GC-SSIM-CRDS*

482

483 Fig. 9 shows good agreement between the calculated and certified $\delta^{13}\text{C}$ values for
484 methane and carbon dioxide after correction. The linearity is highly satisfactory over the full
485 $\delta^{13}\text{C}$ range explored, from -7.2‰ to -40‰ for CO₂ and -23.9 to -66.5‰ for $\delta^{13}\text{C-CH}_4$. These
486 results show the possibility to use a headspace autosampler for the automatization of the
487 calibration procedure.

488

489 *3.5 Application to natural gas samples and comparison with GC-C-IRMS*

490

491 Gas samples collected at several natural gas seep sites of the Marmara sea and
492 characterized by a large range of methane concentrations (between 66 and 99.6 mol% of total
493 gas) were analyzed with the GC-SSIM-CRDS to study the influence of compounds other than
494 methane and carbon dioxide on $\delta^{13}\text{C}$ of the two latter. The results were compared with those
495 obtained from GC-C-IRMS analysis [22]. There is good agreement on the measured $\delta^{13}\text{C-CH}_4$
496 between the two analytical techniques (Table 5), with a maximum RSD of 1.4%. The results
497 also show that the other compounds do not significantly affect the $\delta^{13}\text{C-CH}_4$. For samples
498 denoted ND, it was not possible to measure the $\delta^{13}\text{C-CO}_2$ as their CO_2 concentrations were
499 under 1.1%. Due to multiple assays and losses of samples, there was no more gases available
500 for the analysis of $\delta^{13}\text{C-CH}_4$ for DV3PE3 and for the analysis of $\delta^{13}\text{C-CO}_2$ for Marpegas
501 4/western high (samples denoted NA).

502 Table 6 compares the results of $\delta^{13}\text{C-CO}_2$ measurements carried out with the non-coupled
503 SSIM-CRDS, the GC-SSIM-CRDS and the GC-C-IRMS. It also shows the concentration of
504 CO_2 and CH_4 in ppm measured with the CRDS. The direct analysis of the sample with the
505 SSIM-CRDS without the coupling with the GC leads to very different $\delta^{13}\text{C-CO}_2$ values to those
506 obtained when using the GC-SSIM-CRDS or the GC-C-IRMS; except for the CO_2 -rich sample
507 DV3-PE3. This sample is the only one where CO_2 is largely dominant and exhibits the lowest
508 methane concentration. The four other samples are mainly composed of methane at
509 concentrations ranging between 82.4 and 94.8 mol-%, and such high concentrations make for
510 the unreliable analysis of $\delta^{13}\text{C-CO}_2$ and clearly justify our coupling system GC-SSIM-CRDS.
511 Indeed, the separation step of the GC-SSIM-CRDS makes it possible to obtain reliable $\delta^{13}\text{C-}$
512 CO_2 measurements by avoiding the spectroscopic interferences due to high methane
513 concentration, with accuracy similar to what is achieved with the GC-C-IRMS (Fig. 11). In this
514 example, the difference between the direct injection through the SSIM and the GC-SSIM-

515 CRDS is that a high content of methane interferes in the measurement of $\delta^{13}\text{C}\text{-CO}_2$ even if this
516 gas is defined in the range of 380 to 2000 ppm. By injecting the sample through the GC before,
517 it allows to remove this interference.

518
519
520
521
522
523
524

525 **4 Conclusion**

526

527 We have designed and built a coupled system, the GC-SSIM-CRDS, enabling fast
528 measurement of stable carbon isotope ratios of methane and carbon dioxide, together with the
529 molecular composition of natural gases. This system is transportable and easy-to-use onboard
530 during oceanic cruises. The GC-SSIM-CRDS separates the different components of a natural-
531 gas sample on a packed column, and measures its molecular composition with a thermal
532 conductivity detector. The gas components are sequentially trapped in a loop, avoiding
533 interference effects before being transferred to the SSIM-CRDS for the $\delta^{13}\text{C}$ determination of
534 CH_4 and CO_2 .

535 Several tests have been performed to evaluate the capability of the GC-SSIM-CRDS to
536 accurately measure both isotopic and molecular compositions of natural gases characterized by
537 a wide range of methane and carbon dioxide concentrations. The measured $\delta^{13}\text{C}\text{-CH}_4$ and $\delta^{13}\text{C}\text{-}$
538 CO_2 are in agreement with the values obtained from the commonly applied and well-proven
539 analytical method using a GC-C-IRMS.

540 Besides providing reliable and accurate molecular composition, $\delta^{13}\text{C}\text{-CH}_4$ and $\delta^{13}\text{C}\text{-CO}_2$
541 of natural gases, the GC-SSIM-CRDS can be useful during the exploration step of cruises
542 devoted to the investigation of large-scale gas-emission sites on continental margins and

543 shelves. Indeed, in the context of climate change and its impact on the ocean, and considering
544 the widespread occurrence of gas emissions on continental margins and shelves, the GC-SSIM-
545 CRDS is a valuable tool for decision-making during sampling and onboard analysis. It would
546 thus allow for smart sampling of the gas seeps by identifying the most relevant gas seeps to
547 sample (the ones characterized by gas streams with highly heterogeneous molecular
548 composition, $\delta^{13}\text{C-CH}_4$ and/or $\delta^{13}\text{C-CO}_2$), and would consequently lead to a better
549 understanding of gas sources, transport processes and fates in the ocean.

550

551 **Author contributions**

552 Christophe Brandily designed and built the coupled system, optimized the analytical method,
553 conducted data acquisition and analyses, and wrote the paper. Nolwenn Le Cuff designed and
554 built the coupled system, optimized the analytical method, and conducted data acquisition and
555 analyses. Alexis De Prunele contributed to the optimization of the analytical method for the
556 CRDS. Cécile Cathalot reviewed the paper. Claire Croguennec contributed to the optimization
557 of the analytical method for the CRDS. Jean-Pierre Donval designed and built the coupled
558 system, optimized the analytical method, and conducted data acquisition and analyses. Vivien
559 Guyader designed and built the coupled system, optimized the analytical method, and
560 conducted data acquisition and analyses. Jean-Claude Caprais initiated the acquisition of the
561 CRDS analyzer and developed the methods for this instrument. Livio Ruffine led the Carnot
562 Project, designed the coupled system, interpreted the data and wrote the original draft. Thanks
563 to Alison Chalm for proofreading the article.

564

565 **Declaration of competing interest**

566 The authors declare that they have no known competing financial interests or personal
567 relationships that could influence the work reported in this paper.

568

569 **Acknowledgements**

570 The authors acknowledge the Carnot Institut for the financial support of the project. They also
 571 thank Bertrand Forest (Ifremer, LCSM) for the adaptation of the python software, Pierre
 572 Guyavarch (Ifremer, CTDI) for the Analog to Digital Converter, Laurent Bignon for the shelf
 573 design and the SRA company (Marcy l'Etoile, France) for the GC modified with the valve unit.

574

575 **References**

- 576 [1] M. Saunois, A.R. Stavert, B. Poulter, P. Bousquet, J.G. Canadell, R.B. Jackson, P.A. Raymond, E.J.
 577 Dlugokencky, S. Houweling, P.K. Patra, P. Ciais, V.K. Arora, D. Bastviken, P. Bergamaschi, D.R.
 578 Blake, G. Brailsford, L. Bruhwiler, K.M. Carlson, M. Carrol, S. Castaldi, N. Chandra, C. Crevoisier,
 579 P.M. Crill, K. Covey, C.L. Curry, G. Etiope, C. Frankenberg, N. Gedney, M.I. Hegglin, L. Höglund-
 580 Isaksson, G. Hugelius, M. Ishizawa, A. Ito, G. Janssens-Maenhout, K.M. Jensen, F. Joos, T. Kleinen,
 581 P.B. Krummel, R.L. Langenfelds, G.G. Laruelle, L. Liu, T. Machida, S. Maksyutov, K.C. McDonald, J.
 582 McNorton, P.A. Miller, J.R. Melton, I. Morino, J. Müller, F. Murguía-Flores, V. Naik, Y. Niwa, S.
 583 Noce, S. O'Doherty, R.J. Parker, C. Peng, S. Peng, G.P. Peters, C. Prigent, R. Prinn, M. Ramonet, P.
 584 Regnier, W.J. Riley, J.A. Rosentretter, A. Segers, I.J. Simpson, H. Shi, S.J. Smith, L.P. Steele, B.F.
 585 Thornton, H. Tian, Y. Tohjima, F.N. Tubiello, A. Tsuruta, N. Viovy, A. Voulgarakis, T.S. Weber, M.
 586 van Weele, G.R. van der Werf, R.F. Weiss, D. Worthy, D. Wunch, Y. Yin, Y. Yoshida, W. Zhang, Z.
 587 Zhang, Y. Zhao, B. Zheng, Q. Zhu, Q. Zhu, Q. Zhuang, The Global Methane Budget 2000–2017,
 588 *Earth Syst. Sci. Data*. 12 (2020) 1561–1623. <https://doi.org/10.5194/essd-12-1561-2020>.
- 589 [2] G. Allen, Rebalancing the global methane budget, *Nature*. 538 (2016) 46–48.
 590 <https://doi.org/10.1038/538046a>.
- 591 [3] S. Schwietzke, O.A. Sherwood, L.M.P. Bruhwiler, J.B. Miller, G. Etiope, E.J. Dlugokencky, S.E.
 592 Michel, V.A. Arling, B.H. Vaughn, J.W.C. White, P.P. Tans, Upward revision of global fossil fuel
 593 methane emissions based on isotope database, *Nature*. 538 (2016) 88–91.
 594 <https://doi.org/10.1038/nature19797>.
- 595 [4] P. Bousquet, P. Ciais, J.B. Miller, E.J. Dlugokencky, D.A. Hauglustaine, C. Prigent, G.R. Van der
 596 Werf, P. Peylin, E.-G. Brunke, C. Carouge, R.L. Langenfelds, J. Lathière, F. Papa, M. Ramonet, M.
 597 Schmidt, L.P. Steele, S.C. Tyler, J. White, Contribution of anthropogenic and natural sources to
 598 atmospheric methane variability, *Nature*. 443 (2006) 439–443.
 599 <https://doi.org/10.1038/nature05132>.
- 600 [5] European Commission. Joint Research Centre., Fossil CO₂ and GHG emissions of all world
 601 countries: 2020 report., Publications Office, LU, 2020.
 602 <https://data.europa.eu/doi/10.2760/143674> (accessed April 8, 2021).
- 603 [6] U. Konno, U. Tsunogai, F. Nakagawa, M. Nakaseama, J. Ishibashi, T. Nunoura, K. Nakamura,
 604 Liquid CO₂ venting on the seafloor: Yonaguni Knoll IV hydrothermal system, Okinawa Trough,
 605 *Geophys. Res. Lett.* 33 (2006) L16607. <https://doi.org/10.1029/2006GL026115>.
- 606 [7] E. Suess, Marine cold seeps and their manifestations: geological control, biogeochemical criteria
 607 and environmental conditions, *Int. J. Earth Sci.* 103 (2014) 1889–1916.
 608 <https://doi.org/10.1007/s00531-014-1010-0>.
- 609 [8] A. Boetius, E. Suess, Hydrate Ridge: a natural laboratory for the study of microbial life fueled by
 610 methane from near-surface gas hydrates, *Geomicrobiol. Biogeochem. Gas Hydrates Hydrocarb.*
 611 *Seeps*. 205 (2004) 291–310. <https://doi.org/10.1016/j.chemgeo.2003.12.034>.

- 612 [9] M. Sibuet, K.O.-L. Roy, Cold Seep Communities on Continental Margins: Structure and
613 Quantitative Distribution Relative to Geological and Fluid Venting Patterns, in: G. Wefer, D.
614 Billett, D. Hebbeln, B.B. Jørgensen, M. Schlüter, T.C.E. van Weering (Eds.), *Ocean Margin Syst.*,
615 Springer Berlin Heidelberg, Berlin, Heidelberg, 2002: pp. 235–251. https://doi.org/10.1007/978-3-662-05127-6_15.
- 617 [10] M. Sibuet, K. Olu, Biogeography, biodiversity and fluid dependence of deep-sea cold-seep
618 communities at active and passive margins, *Deep Sea Res. Part II Top. Stud. Oceanogr.* 45 (1998)
619 517–567. [https://doi.org/10.1016/S0967-0645\(97\)00074-X](https://doi.org/10.1016/S0967-0645(97)00074-X).
- 620 [11] D.L. Valentine, Emerging Topics in Marine Methane Biogeochemistry, *Annu. Rev. Mar. Sci.* 3
621 (2011) 147–171. <https://doi.org/10.1146/annurev-marine-120709-142734>.
- 622 [12] M.J. Whiticar, Carbon and hydrogen isotope systematics of bacterial formation and oxidation of
623 methane, *Chem. Geol.* 161 (1999) 291–314. [https://doi.org/10.1016/S0009-2541\(99\)00092-3](https://doi.org/10.1016/S0009-2541(99)00092-3).
- 624 [13] M. Whiticar, Correlation of Natural Gases with Their Sources: Chapter 16: Part IV. Identification
625 and Characterization, in: 1994.
- 626 [14] M. Schoell, Multiple origins of methane in the Earth, *Chem. Geol.* 71 (1988) 1–10.
627 [https://doi.org/10.1016/0009-2541\(88\)90101-5](https://doi.org/10.1016/0009-2541(88)90101-5).
- 628 [15] M.J. Whiticar, E. Faber, Methane oxidation in sediment and water column environments—
629 Isotope evidence, *Org. Geochem.* 10 (1986) 759–768. [https://doi.org/10.1016/S0146-6380\(86\)80013-4](https://doi.org/10.1016/S0146-6380(86)80013-4).
- 631 [16] L. Ruffine, J.-P. Donval, C. Croguennec, P. Burnard, H. Lu, Y. Germain, L.N. Legoix, L. Bignon, M.N.
632 Çağatay, B. Marty, D. Madre, M. Pitel-Roudaut, P. Henry, L. Géli, Multiple gas reservoirs are
633 responsible for the gas emissions along the Marmara fault network, *Deep Sea Res. Part II Top.*
634 *Stud. Oceanogr.* 153 (2018) 48–60. <https://doi.org/10.1016/j.dsr2.2017.11.011>.
- 635 [17] J.L. Lewicki, C.M. Oldenburg, L. Dobeck, L. Spangler, Surface CO₂ leakage during two shallow
636 subsurface CO₂ releases, *Geophys. Res. Lett.* 34 (2007) L24402.
637 <https://doi.org/10.1029/2007GL032047>.
- 638 [18] P.R. Dando, S. Aliani, H. Arab, C.N. Bianchi, M. Brehmer, S. Cocito, S.W. Fowlers, J. Gundersen,
639 L.E. Hooper, R. Kölbh, J. Kuevere, P. Linke, K.C. Makropoulos, R. Meloni, J.-C. Miquel, C. Morri, S.
640 Müller, C. Robinson, H. Schlesner, S. Sieverts, R. Störr, D. Stüben, M. Thormm, S.P. Varnavas, W.
641 Ziebiss, Hydrothermal studies in the aegean sea, *Phys. Chem. Earth Part B Hydrol. Oceans*
642 *Atmosphere.* 25 (2000) 1–8. [https://doi.org/10.1016/S1464-1909\(99\)00112-4](https://doi.org/10.1016/S1464-1909(99)00112-4).
- 643 [19] A. Aiuppa, A. Caleca, C. Federico, S. Gurrieri, M. Valenza, Diffuse degassing of carbon dioxide at
644 Somma–Vesuvius volcanic complex (Southern Italy) and its relation with regional tectonics, *J.*
645 *Volcanol. Geotherm. Res.* 133 (2004) 55–79. [https://doi.org/10.1016/S0377-0273\(03\)00391-3](https://doi.org/10.1016/S0377-0273(03)00391-3).
- 646 [20] K. Gürgey, R.P. Philp, C. Clayton, H. Emiroğlu, M. Siyako, Geochemical and isotopic approach to
647 maturity/source/mixing estimations for natural gas and associated condensates in the Thrace
648 Basin, NW Turkey, *Appl. Geochem.* 20 (2005) 2017–2037.
649 <https://doi.org/10.1016/j.apgeochem.2005.07.012>.
- 650 [21] H. Wycherley, A. Fleet, H. Shaw, Some observations on the origins of large volumes of carbon
651 dioxide accumulations in sedimentary basins, *Mar. Pet. Geol.* 16 (1999) 489–494.
652 [https://doi.org/10.1016/S0264-8172\(99\)00047-1](https://doi.org/10.1016/S0264-8172(99)00047-1).
- 653 [22] Jin-xing Dai, Yan Song, Chun-sen Da, Geochemistry and Accumulation of Carbon Dioxide Gases in
654 China, *AAPG Bull.* 80 (1996). <https://doi.org/10.1306/64EDA0D2-1724-11D7-8645000102C1865D>.
- 656 [23] D.F. McGinnis, M. Schmidt, T. DelSontro, S. Themann, L. Rovelli, A. Reitz, P. Linke, Discovery of a
657 natural CO₂ seep in the German North Sea: implications for shallow dissolved gas and seep
658 detection, *J. Geophys. Res.* 116 (2011) C03013. <https://doi.org/10.1029/2010JC006557>.
- 659 [24] B. Bernard, J.M. Brooks, W.M. Sackett, A geochemical model for characterization of hydrocarbon
660 gas sources in marine sediments., 9 Th Annu. OTC Conf. (1977) 435–438.
- 661 [25] Schoell, Genetic characterization of natural gases, *Am. Assoc. Pet. Geol. Bull.* 67 (1983) 2225–
662 2238.
- 663 [26] M.J. Whiticar, E. Faber, M. Schoell, Biogenic methane formation in marine and freshwater

- 664 environments: CO₂ reduction vs. acetate fermentation—Isotope evidence, *Geochim.*
665 *Cosmochim. Acta.* 50 (1986) 693–709. [https://doi.org/10.1016/0016-7037\(86\)90346-7](https://doi.org/10.1016/0016-7037(86)90346-7).
- 666 [27] L.K. Gutsalo, A.M. Plotnikov, Carbon isotopic composition in the CO₂-CH₄ system as a criterion
667 for the origin of methane and carbon dioxide in Earth natural gases., *Dokl. Akad. Nauk SSSR.* 259
668 (1981).
- 669 [28] A.V. Milkov, G. Etiope, Revised genetic diagrams for natural gases based on a global dataset of
670 >20,000 samples, *Org. Geochem.* 125 (2018) 109–120.
671 <https://doi.org/10.1016/j.orggeochem.2018.09.002>.
- 672 [29] L. Ruffine, H. Ondreas, M.-M. Blanc-Valleron, B.M.A. Teichert, C. Scalabrin, E. Rinnert, D. Birot, C.
673 Croguennec, E. Ponzevera, C. Pierre, J.-P. Donval, A.-S. Alix, Y. Germain, L. Bignon, J. Etoubleau,
674 J.-C. Caprais, J. Knoery, F. Lesongeur, B. Thomas, A. Roubi, L.N. Legoix, P. Burnard, N. Chevalier,
675 H. Lu, S. Dupré, C. Fontanier, D. Dissard, N. Olgun, H. Yang, H. Strauss, V. Özaksoy, J. Perchoc, C.
676 Podeur, C. Tarditi, E. Özbeki, V. Guyader, B. Marty, D. Madre, M. Pitel-Roudaut, C. Grall, D.
677 Embriaco, A. Polonia, L. Gasperini, M.N. Çağatay, P. Henry, L. Géli, Multidisciplinary investigation
678 on cold seeps with vigorous gas emissions in the Sea of Marmara (MarsiteCruise): Strategy for
679 site detection and sampling and first scientific outcome, *Deep Sea Res. Part II Top. Stud.*
680 *Oceanogr.* 153 (2018) 36–47. <https://doi.org/10.1016/j.dsr2.2018.03.006>.
- 681 [30] M. Miró, P. Worsfold, C. Poole, A. Townshend, *Encyclopedia of analytical science. Volume 1*
682 *Volume 1*, 2019.
683 [http://search.ebscohost.com/login.aspx?direct=true&scope=site&db=nlebk&db=nlabk&AN=186](http://search.ebscohost.com/login.aspx?direct=true&scope=site&db=nlebk&db=nlabk&AN=1866138)
684 [6138](http://search.ebscohost.com/login.aspx?direct=true&scope=site&db=nlebk&db=nlabk&AN=1866138) (accessed October 5, 2020).
- 685 [31] W. Meier-Augenstein, Applied gas chromatography coupled to isotope ratio mass spectrometry,
686 *J. Chromatogr. A.* 842 (1999) 351–371. [https://doi.org/10.1016/S0021-9673\(98\)01057-7](https://doi.org/10.1016/S0021-9673(98)01057-7).
- 687 [32] D.E. Matthews, J.M. Hayes, Isotope-ratio-monitoring gas chromatography-mass spectrometry,
688 *Anal. Chem.* 50 (1978) 1465–1473. <https://doi.org/10.1021/ac50033a022>.
- 689 [33] N.L. Miles, D.K. Martins, S.J. Richardson, C.W. Rella, C. Arata, T. Lauvaux, K.J. Davis, Z.R. Barkley,
690 K. McKain, C. Sweeney, Calibration and field testing of cavity ring-down laser spectrometers
691 measuring CH₄, CO₂, and δ¹³CH₄ deployed on towers in the Marcellus Shale region,
692 *Atmospheric Meas. Tech.* 11 (2018) 1273–1295. <https://doi.org/10.5194/amt-11-1273-2018>.
- 693 [34] H.M. Roberts, A.M. Shiller, Determination of dissolved methane in natural waters using
694 headspace analysis with cavity ring-down spectroscopy, *Anal. Chim. Acta.* 856 (2015) 68–73.
695 <https://doi.org/10.1016/j.aca.2014.10.058>.
- 696 [35] E.R. Crosson, A cavity ring-down analyzer for measuring atmospheric levels of methane, carbon
697 dioxide, and water vapor, *Appl. Phys. B.* 92 (2008) 403–408. [https://doi.org/10.1007/s00340-](https://doi.org/10.1007/s00340-008-3135-y)
698 [008-3135-y](https://doi.org/10.1007/s00340-008-3135-y).
- 699 [36] L. Ruffine, J.-P. Donval, C. Croguennec, L. Bignon, D. Birot, A. Battani, G. Bayon, J.-C. Caprais, N.
700 Lantéri, D. Levaché, S. Dupré, Gas Seepage along the Edge of the Aquitaine Shelf (France): Origin
701 and Local Fluxes, *Geofluids.* 2017 (2017) 1–13. <https://doi.org/10.1155/2017/4240818>.
- 702 [37] S. Assan, A. Baudic, A. Guemri, P. Ciais, V. Gros, F.R. Vogel, Characterization of interferences to in
703 situ observations of δ¹³CH₄ and C₂H₆ when using a cavity ring-down spectrometer at industrial
704 sites, *Atmospheric Meas. Tech.* 10 (2017) 2077–2091. [https://doi.org/10.5194/amt-10-2077-](https://doi.org/10.5194/amt-10-2077-2017)
705 [2017](https://doi.org/10.5194/amt-10-2077-2017).
- 706 [38] H. Nara, H. Tanimoto, Y. Tohjima, H. Mukai, Y. Nojiri, K. Katsumata, C.W. Rella, Effect of air
707 composition (N₂, O₂, Ar, and
708 H₂O) on CO₂ and CH₄
709 measurement by wavelength-scanned cavity ring-down spectroscopy: calibration and
710 measurement strategy, *Atmospheric Meas. Tech.* 5 (2012) 2689–2701.
711 <https://doi.org/10.5194/amt-5-2689-2012>.
- 712 [39] G. Friedrichs, J. Bock, F. Temps, P. Fietzek, A. Körtzinger, D.W.R. Wallace, Toward continuous
713 monitoring of seawater ¹³CO₂/¹²CO₂ isotope ratio and pCO₂: Performance of cavity ringdown
714 spectroscopy and gas matrix effects, *Limnol. Oceanogr. Methods.* 8 (2010) 539–551.
715 <https://doi.org/10.4319/lom.2010.8.539>.

- 716 [40] K. Malowany, J. Stix, A. Van Pelt, G. Lucic, H₂S interference on CO₂ isotopic measurements using
 717 a Picarro G1101-i cavity ring-down spectrometer, *Atmospheric Meas. Tech.* 8 (2015) 4075–4082.
 718 <https://doi.org/10.5194/amt-8-4075-2015>.
- 719 [41] C.W. Rella, J. Hoffnagle, Y. He, S. Tajima, Local- and regional-scale measurements of CH₄,
 720 δ¹³CH₄, and C₂H₆ in the Uintah Basin using a mobile stable isotope analyzer, *Atmospheric*
 721 *Meas. Tech.* 8 (2015) 4539–4559. <https://doi.org/10.5194/amt-8-4539-2015>.
- 722 [42] Picarro Inc, Picarro G2201-i CRDS analyzer for isotopic carbon in CO₂ and CH₄, (2015).
- 723 [43] J.P. Donval, V. Guyader, E. Boissy, A simple method for the preparation and injection of gas
 724 mixtures into a gas chromatograph using a two-component device, *J. Chromatogr. A.* (2020)
 725 461579. <https://doi.org/10.1016/j.chroma.2020.461579>.
- 726 [44] R.N. Zare, D.S. Kuramoto, C. Haase, S.M. Tan, E.R. Crosson, N.M.R. Saad, High-precision optical
 727 measurements of ¹³C/¹²C isotope ratios in organic compounds at natural abundance, *Proc. Natl.*
 728 *Acad. Sci.* 106 (2009) 10928–10932. <https://doi.org/10.1073/pnas.0904230106>.
- 729 [45] N. Lanteri, L. Bignon, J. Dupont, Device for taking pressurized samples, EP2010886B1, 2011.
- 730 [46] J.L. Charlou, J.P. Donval, Y. Fouquet, H. Ondreas, J. Knoery, P. Cochonat, D. Levaché, Y. Poirier, P.
 731 Jean-Baptiste, E. Fourré, B. Chazallon, Physical and chemical characterization of gas hydrates and
 732 associated methane plumes in the Congo–Angola Basin, *Chem. Geol.* 205 (2004) 405–425.
 733 <https://doi.org/10.1016/j.chemgeo.2003.12.033>.
- 734 [47] D.H. Doehlert, Uniform Shell Designs, *Appl. Stat.* 19 (1970) 231.
 735 <https://doi.org/10.2307/2346327>.
- 736 [48] S.L.C. Ferreira, W.N.L. dos Santos, C.M. Quintella, B.B. Neto, J.M. Bosque-Sendra, Doehlert
 737 matrix: a chemometric tool for analytical chemistry—review, *Talanta.* 63 (2004) 1061–1067.
 738 <https://doi.org/10.1016/j.talanta.2004.01.015>.
- 739 [49] J.P. Donval, V. Guyader, Analysis of hydrogen and methane in seawater by “Headspace” method:
 740 Determination at trace level with an automatic headspace sampler, *Talanta.* 162 (2017) 408–414.
 741 <https://doi.org/10.1016/j.talanta.2016.10.034>.
- 742 [50] L.E. McHale, A. Hecobian, A.P. Yalin, Open-path cavity ring-down spectroscopy for trace gas
 743 measurements in ambient air, *Opt. Express.* 24 (2016) 5523.
 744 <https://doi.org/10.1364/OE.24.005523>.
- 745 [51] R.S. Brown, I. Kozin, Z. Tong, R.D. Oleschuk, H.-P. Loock, Fiber-loop ring-down spectroscopy, *J.*
 746 *Chem. Phys.* 117 (2002) 10444–10447. <https://doi.org/10.1063/1.1527893>.
- 747 [52] J. Pang, X. Wen, X. Sun, K. Huang, Intercomparison of two cavity ring-down spectroscopy
 748 analyzers for atmospheric ¹³CO₂/¹²CO₂ measurement, *Atmospheric Meas. Tech.* 9 (2016) 3879–
 749 3891. <https://doi.org/10.5194/amt-9-3879-2016>.
- 750 [53] N.V. Tsederberg, *Thermal Conductivity of Gases and Liquids*, Cambridge, MA, USA, 1965.

751
 752

753 **Table captions**

754

755 Table 1. Analytical conditions applied to the GC and the V_i and V_t valves.

756

757 Table 2. Commercial Certified δ¹³C-CH₄ and δ¹³C-CO₂ gas standards used for this study.

758 Table 3. Statistic test of δ¹³C-CH₄ with the [CH₄] (ppm) variations for the HR mode with z the

759 average from 10 replicates, NE the normalized error, U the uncertainty, uref the uncertainty

760 from the reference value, MB the maximal bias and ref the isotopic certified value.

761

762 Table 4. Limits of concentration for the gas samples injected into the GC-SSIM-CRDS with a
763 1 mL injection loop and the gas injector

764

765 Table 5. Comparison of $\delta^{13}\text{C-CH}_4$ and $\delta^{13}\text{C-CO}_2$ measured with the SSIM-CRDS and the GC-
766 C-IRMS for 16 natural gases. Gases compositions (% mol) were determined in previous
767 studies.

768

769 Table 6. Comparison between the GC-SSIM-CRDS, the SSIM-CRDS and GC-C-IRMS
770 measurements of $\delta^{13}\text{C-CO}_2$ for 5 natural gas samples from the Marmara sea. Gases
771 compositions (% mol) were determined in previous studies.

772

773

774

775 **Figure captions**

776

777 Fig. 1. Schematic overview of the coupled system: Gas Chromatography 6850 Agilent
778 implemented with an 8-port valve, Vt, connected to SSIM-CRDS. A head-space sampler or a
779 gas tight syringe can be coupled to the GC using the purge packed inlet injector (PPI).

780

781 Fig. 2. Photo of the GC-SSIM-CRDS.

782

783 Fig. 3. Chromatogram of the trapping and subsequent $\delta^{13}\text{C}$ analysis of methane and carbon
784 dioxide by switching from one position to another. (a) Vt OFF: the CO_2 is trapped in the loop
785 during the $\delta^{13}\text{C-CH}_4$ measurement; (b) Vt ON: the CO_2 is delivered to the SSIM-CRDS for the
786 measurement of its $\delta^{13}\text{C}$.

787

788 Fig. 4. Variation of $\delta^{13}\text{C-CH}_4$ with CH_4 concentration (ppm) in the HR mode from 29 sample

789 injections of the standard at of -38.3‰ ($\pm 0.2\text{‰}$) of $\delta^{13}\text{C-CH}_4$. σ_p represents the standard
790 deviation reported by Picarro.

791

792 Fig. 5. Fluctuation of $\delta^{13}\text{C-CO}_2$ with the reciprocal CO_2 concentration for each of the four
793 certified standards.

794

795 Fig. 6. Influence of concentration of the injected CO_2 on $\delta^{13}\text{C-CO}_2$ calibration.

796

797 Fig. 7. A_N and B_N plots versus $1/[\text{CO}_2]$.

798

799 Fig. 8. Chromatogram of CH_4 and CO_2 in a mixture of C1 to C5.

800

801 Fig. 9. Calibration curve obtained with the GC-SSIM-CRDS for $\delta^{13}\text{C-CH}_4$ and $\delta^{13}\text{C-CO}_2$ for 5
802 replications.

803

804 Fig. 10. Graph showing the good agreement on the $\delta^{13}\text{C-CH}_4$ values measured with the SSIM-
805 CRDS and the GC-C-IRMS for 16 natural gas samples.

806

807

808 Fig. 11. Comparison between $\delta^{13}\text{C-CO}_2$ values measured with the GC-SSIM-CRDS and the
809 GC-C-IRMS for 4 natural gas samples. The concentrations of CO_2 and CH_4 in mol% were
810 determined previously (not with this system).

811

Journal Pre-proof

Table 1

Injection valve box		
Sample loop size	0.1 and 1 mL	
Temperature	32 °C	
Column		
Type	Shincarbon (ST 80/100, 2m x 3mm)	
Flow	6 mL min ⁻¹	
Temperature	184 °C	
μTCD		
Temperature	250 °C	
Reference flow	9 mL min ⁻¹	
Valve	time	Position
Vi	0 min	off
Vt	3.2 min	on
Vt	3.6 min	off
Vt	4.3 min	on
Vt	13 min	off
Vi	13 min	on

Table 2

Gas	Standard	Origin	[gas] mol% in air balance	$\delta^{13}\text{C}$ vs PDB ‰	$\pm\sigma$ ‰
CO ₂	CLM-3783-10 High level Gas	Cambridge isotope laboratories	5	-7.12	0.4
	CLM-9026-10 Mid level Gas		5	-13.51	0.5
	CLM-3781-10 Baseline Calibrant Gas		5	-22.62	0.2
	UN1956	AirGas (Air Liquide)	50	-40.1	0.3
CH ₄	L-iso1	Isometric instrument	0.25	-66.5	0.2
	B-iso1		0.25	-54.5	0.2
	T-iso1		0.25	-38.3	0.2
	H-iso1		0.25	-23.9	0.2

813 Table 3

814

$\delta^{13}\text{C-CO}_2$ ‰	ref+uref ‰	ref-uref ‰	ref+MB ‰	ref-MB ‰	[CO ₂] ppm	U	z ‰	NE
					55	0.4	-66.44	0.33
-66.5	-66.3	-66.7	-65.7	-67.3	542	0.4	-66.45	0.45
					1015	0.4	-66.34	0.80
					55	0.4	-54.45	0.25
-54.5	-54.3	-54.7	-53.7	-55.3	545	0.4	-54.50	0.41
					1023	0.4	-54.38	0.55
					55	0.4	-38.31	0.05
-38.3	-38.1	-38.5	-37.5	-39.1	533	0.4	-38.40	0.76
					1011	0.5	-38.24	0.27
					55	0.4	-23.83	0.32
-23.9	-23.7	-24.1	-23.1	-24.7	541	0.4	-23.80	0.55
					1021	0.4	-23.77	1.56

815

816

817 Table 4

818

Compound	Limit of detection (% mol) on the GC	Low gas concentration limit (% mol) to inject for isotopy	High gas concentration limit (% mol) to inject for isotopy	maximum amount of gas (nmol) to inject on the GC for isotopy
CH ₄	0.0006	0.14 for HR and 0.010 for HP	5.4	2200
CO ₂	0.0030	1.1	4.4	1800

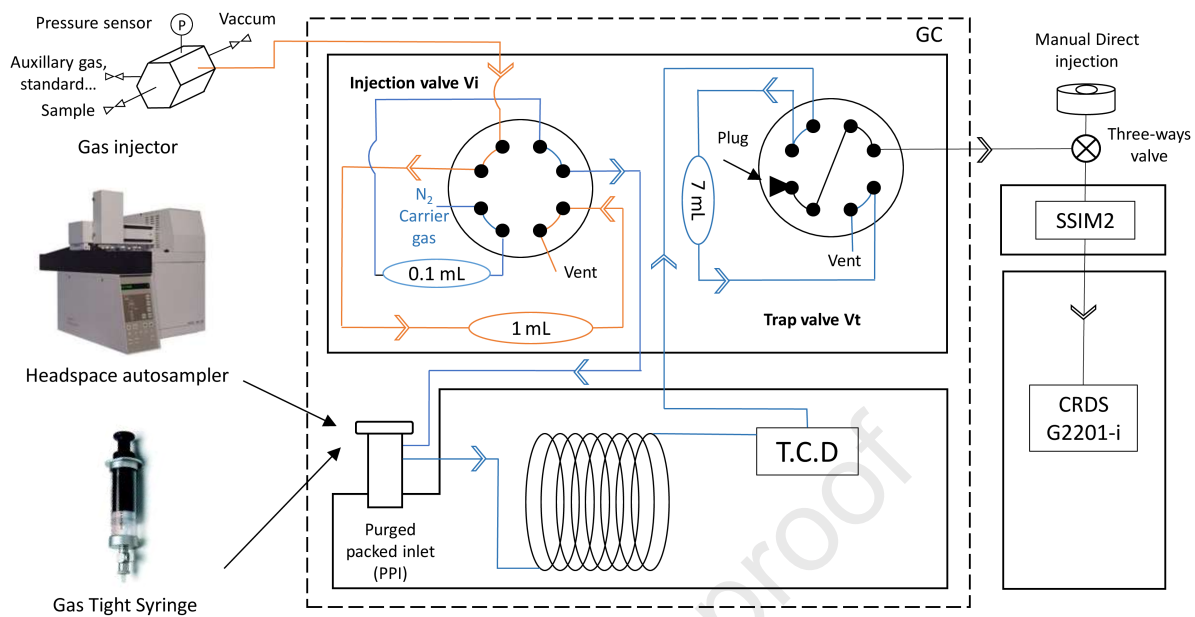
819

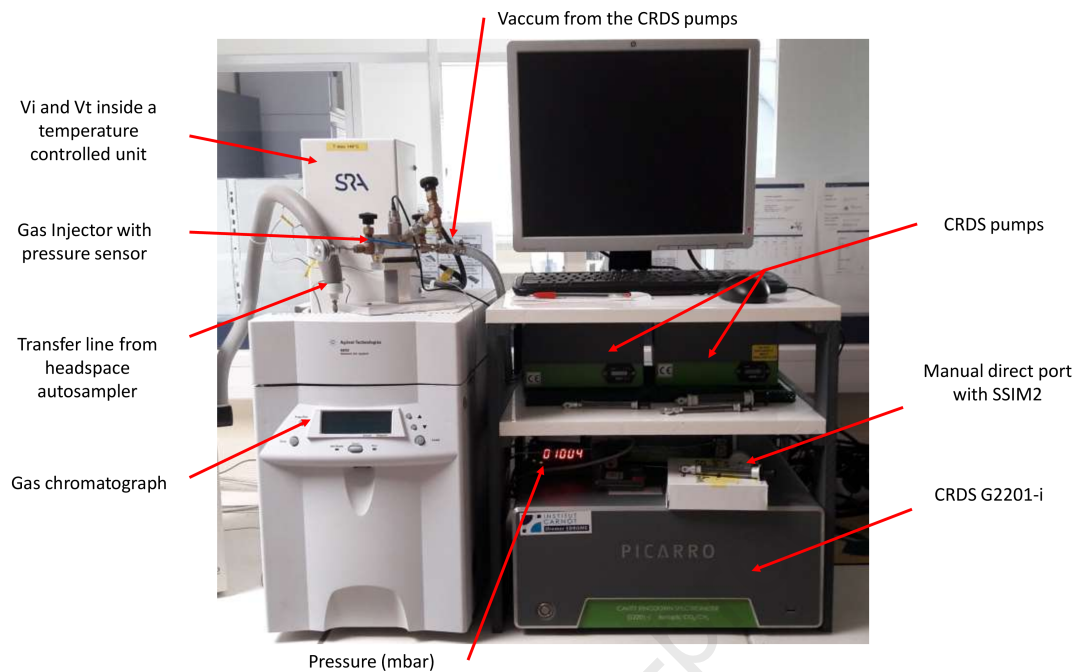
Table 5

Cruise/Sample name		% mol (previously determined)					$\delta^{13}\text{C}$ ‰ CH ₄ GC- CRDS	$\delta^{13}\text{C}$ -CH ₄ ‰ GC-C-IRMS Isolab	$\delta^{13}\text{C}$ ‰ CO ₂ GC- CRDS	$\delta^{13}\text{C}$ -CO ₂ ‰ GC-C-IRMS Isolab
		methane	C ₂ +	Carbon dioxide	Nitrogen	Hydrogen sulfide				
Marsite 2014	MRS-DV1-PE02	98,71	0,49	0,55	0,25	0	-44,1	-43,5	ND	ND
	MRS-DV1-PE03	98,65	0,85	0,14	0,36	0	-53	-53	ND	ND
	MRS-DV2-PE02	82,39	9,01	8,6	0	0	-43,5	-44	28,3	28,4
	MRS-DV3-PE01	94,76	3,44	1,59	0,21	0,18	-52,1	-52,3	11,8	12
	MRS-DV3-PE06	94,48	3,39	1,95	0,18	0,1	-52,1	-52,2	17,6	16,9
	MRS-DV3-PE09	99,53	0,13	0,11	0,22	0,07	-58	-58,4	ND	ND
	MRS-DV4-PE02	99,79	0,01	0,1	0,1	0	-64,1	-63,8	ND	ND
	MRS-DV4-PE07	99,67	0,01	0,09	0,24	0	-65,8	-66,1	ND	ND
	MRS-DV4-PE08	99,53	0,02	0,09	0,36	0,02	-65,8	-66	ND	ND
	DV3-PE3	2,01	9	97,64	0,2	0	NA	-34	-3,5	-3,7
	MRS-DV5-PE01	99,68	0,01	0,14	0,17	0	-63,4	-63,5	ND	ND
	MRS-DV5-PE02	99,74	0,01	0,13	0,12	0	-62,6	-63,1	ND	ND
	MRS-DV5-PE03	99,74	0,01	0,09	0,16	0	-63,6	-63,8	ND	ND
	MRS-DV5-PE04	99,61	0,09	0,18	0,11	0,02	-62	-62,1	ND	ND
Marpegas1 / Central High		98,86	0,52	0,36	0,26	NA	-44,2	-44,4	ND	ND
Marpegas4 / Western High		90,90	5,2	3,9	0	NA	-44,6	-44,4	NA	NA
Marpegas5 / Cinarcik Basin		99,63	0,01	0,1	0,26	NA	-64	-64,1	ND	ND

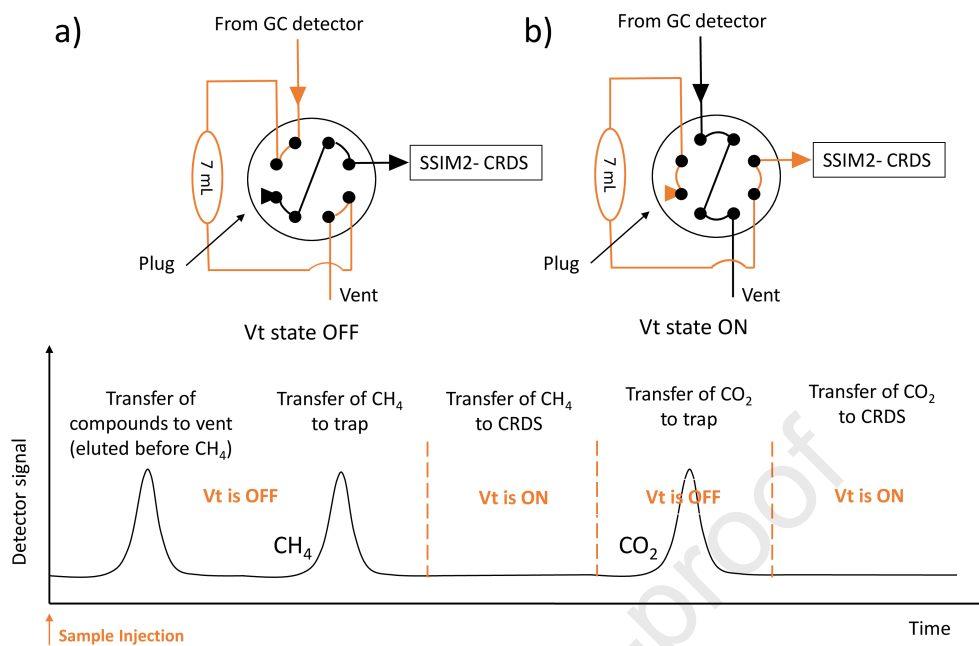
Table 6

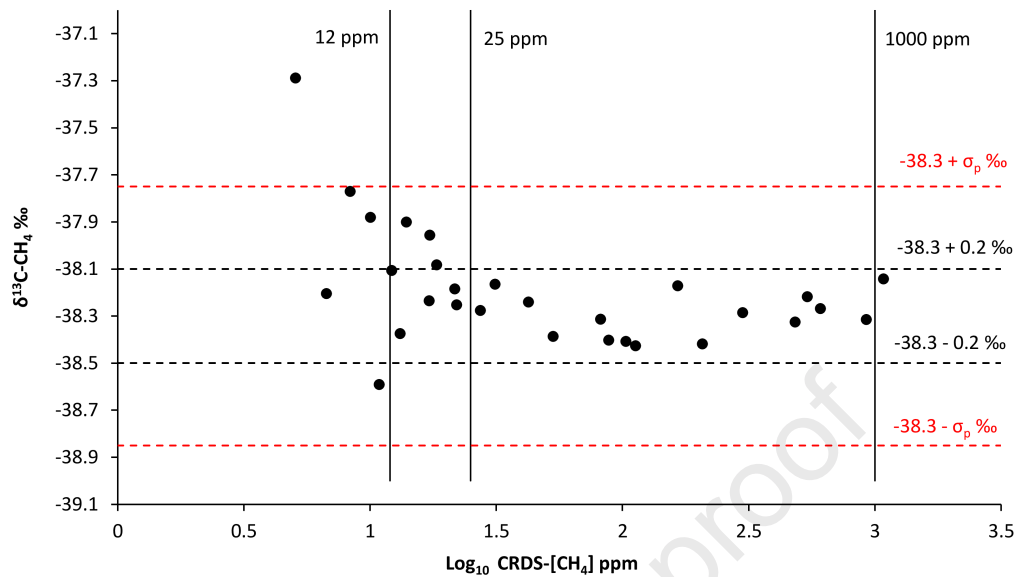
Sample	GC-SSIM- CRDS/ ‰	IRMS ‰	SSIM- CRDS ‰	[CO ₂] CRDS ppm	[CH ₄] CRDS ppm	CO ₂ mol %	CH ₄ mol %
DV2-PE2	+28.3	+28.4	+2806	592	8030	8.60	82.39
DV3-PE3	-3.5	-3.7	-3.78	1101	26.1	97.64	2.01
DV3 PE01	+11.8	+12.0	+11287	552	33463	1.59	94.76
DV3 PE06	+17.6	+16.9	+9606	548	26676	1.95	94.48

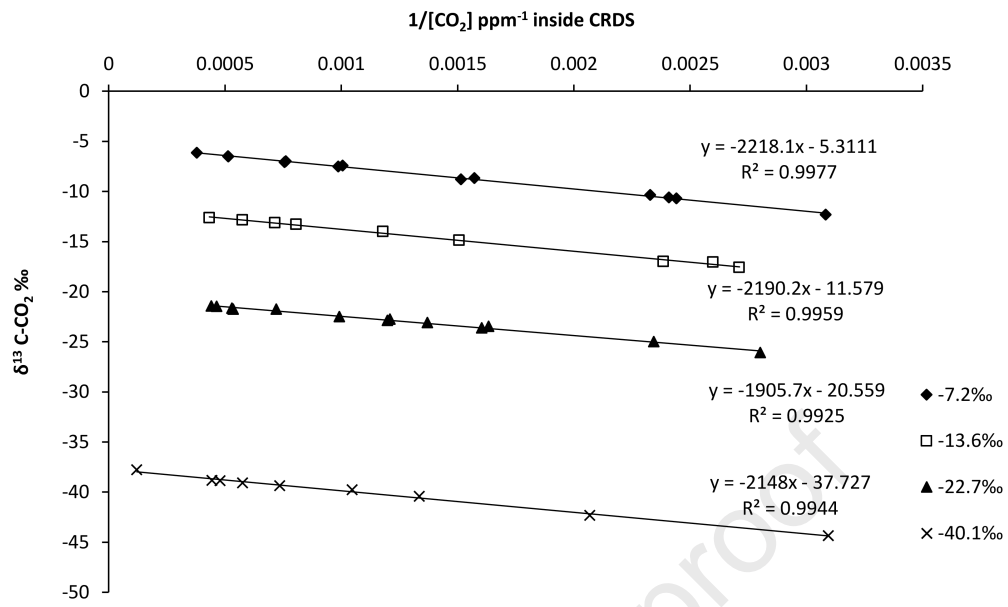


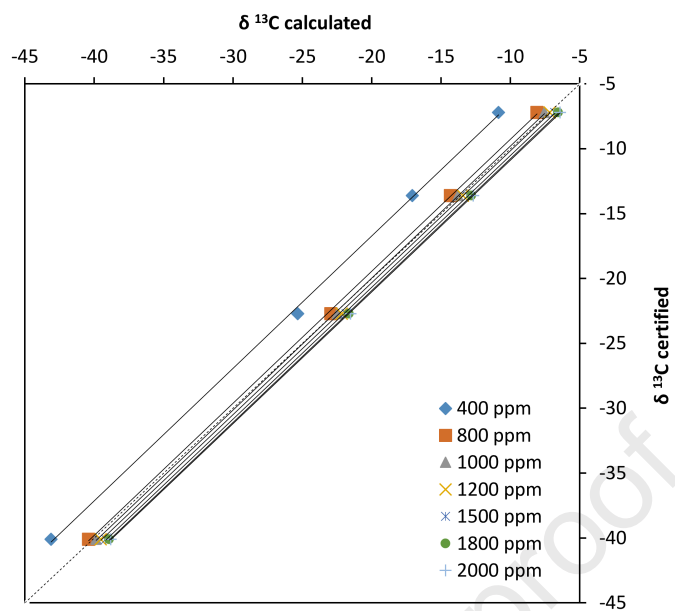


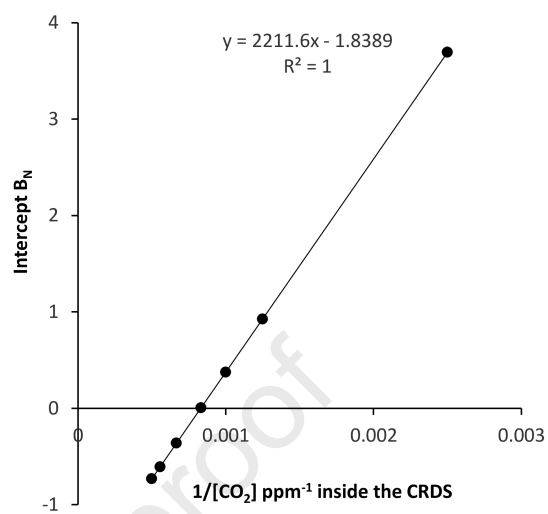
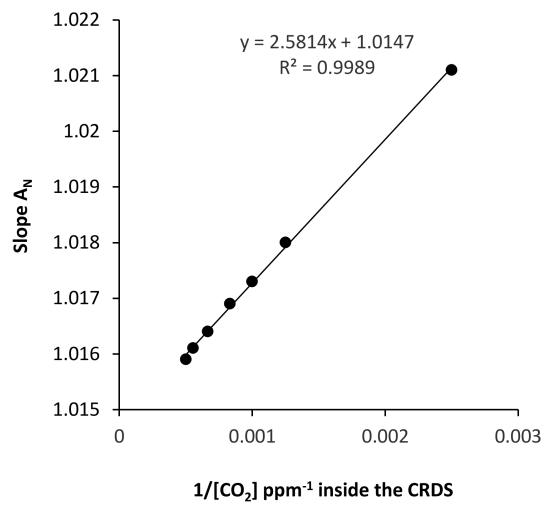
Journal Pre-proof

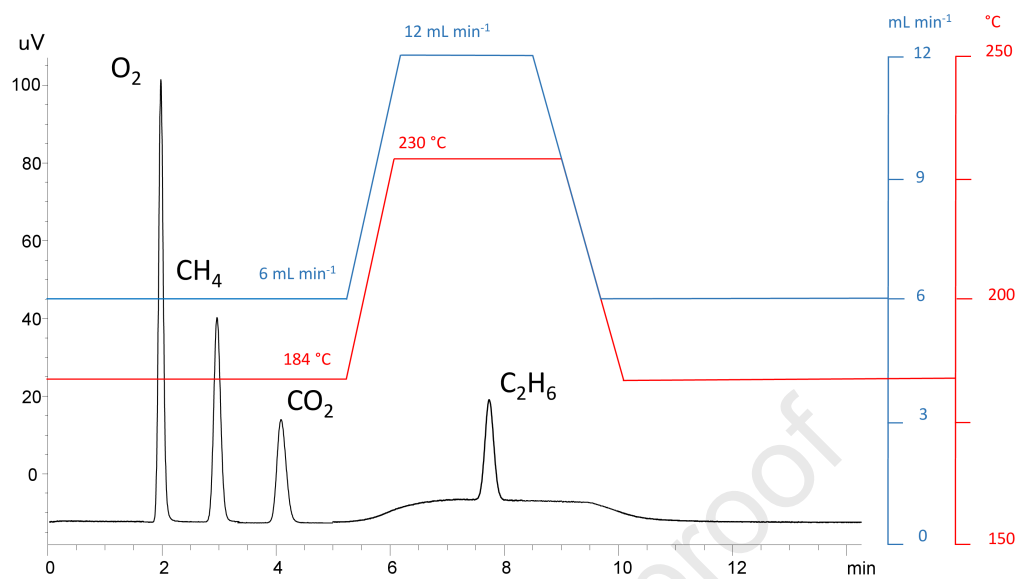


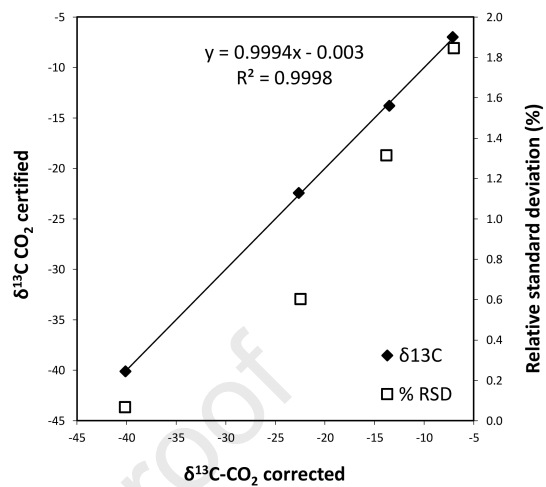
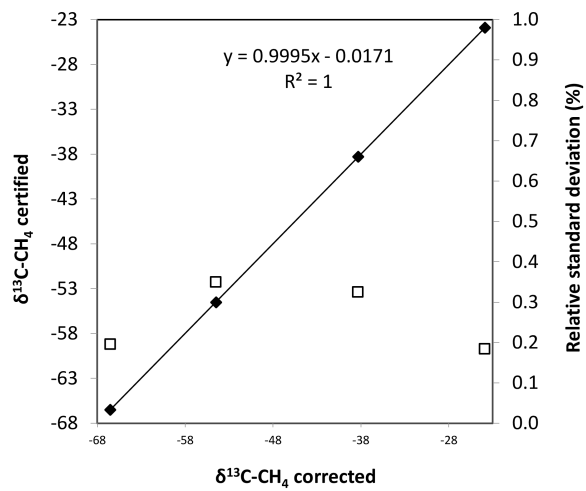


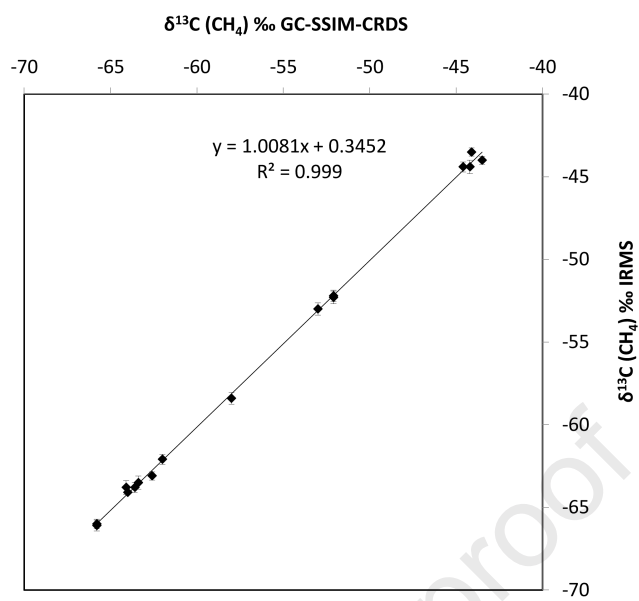


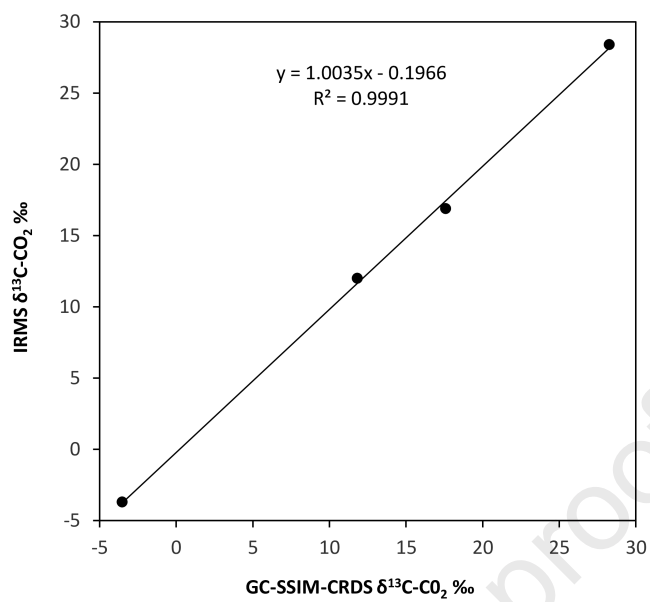












Highlights:

- We present a coupled analytical system associating gas chromatography and cavity ring down spectroscopy (GC-SSIM-CRDS) for natural gas analyses
- The analytical system allows fast onboard analyses of both molecular composition of natural gases and stable carbon isotope ratios of methane and carbon dioxide in 24 min.
- The GC-SSIM-CRDS was optimized and validated with samples from natural gas seeps
- The GC-SSIM-CRDS is a decision-making tool suitable to refining sampling strategy of gases when characterizing seep areas and is a useful analytical system for scientific purposes.

Declaration of interests

The authors declare that they have no known competing financial interests or personal relationships that could have appeared to influence the work reported in this paper.

The authors declare the following financial interests/personal relationships which may be considered as potential competing interests:

Journal Pre-proof